34th Annual International Conference of the IEEE EMBS
San Diego, California USA, 28 August - 1 September, 2012

# Analysis of Tight Junction Formation and Integrity*

Mahmut Karakaya, Ryan A. Kerekes, Jennifer L. Morrell-Falvey, Carmen M. Foster, and Scott T. Retterer

*Abstract*— **In this paper, we study segmentation of tight junctions and analyze the formation and integrity of tight junctions in large-scale confocal image stacks, a challenging biological problem because of the low spatial resolution images and the presence of breaks in tight junction structure. We present an automated, three-step processing approach for tight junction analysis. In our approach, we first localize each individual nucleus in the image by using thresholding, morphological filters and active contours. By using each nucleus position as a seed point, we automatically segment the cell body based on the active contour. We then use an intensity-based skeletonization algorithm to generate the boundary regions for each cell, and features are extracted from tight junctions associated with each cell to assess tight junction continuity. Based on qualitative results and quantitative comparisons, we show that we are able to automatically segment tight junctions and compute relevant features that provide a quantitative measure of tight junction formation to which the permeability of the cell monolayer can ultimately be correlated.**

## I. Introduction

Over the past decade, recent advances in cellular imaging technology have made it possible to capture high-resolution images of cellular structures and processes that enable biologists to investigate fundamental questions in cell structure, morphological development, and cellular disorders. One dynamic structure of interest is the blood-brain barrier (BBB), a selective barrier formed by epithelial cells that is highly restrictive in the transport of substances between the blood and the central nervous system [1]. The epithelial cells found in the BBB form complex tight junctions by the interaction of several transmembrane proteins, such as occludin and claudin, which effectively seal the paracellular space. Paracellular transport can be regulated in response to different conditions, in part through the action of accessory proteins, such as ZO-1, which link transmembrane proteins to the actin cytoskeleton. Disruptions in BBB barrier function have been implicated in several neurodegenerative disorders and can be a consequence of stroke and traumatic brain injury [2]. In vitro systems are needed to understand how the formation and regulation of tight junction structures ultimately affect permeability and transport across the BBB. These data will provide much needed insights for effective drug design and models of disease progression.

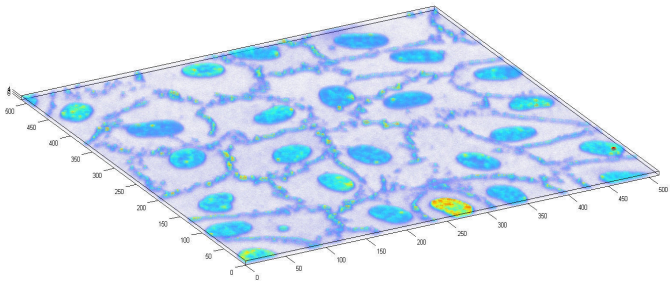

Figure 1. 3D image of nucleus and tight junction protein ZO-1. 25 cells are visible with differing tight junction morphologies.

With the use of epithelial cell lines and immunofluorescence methods, it is possible to collect detailed three dimensional images of tight junction structures using confocal laser scanning microscopy. However, computational methods to analyze these cell structures have not kept pace with imaging technology, and biologists still rely largely on manual analysis procedures which are laborious and time-consuming. Therefore, the automatic analysis of cell structure from image reconstructions of tight junctions is essential to fully extract the data found in these valuable sources.

In this paper, we propose a method to segment and quantify disruptions or breaks in tight junctions from maximum intensity projections of optical sections acquired using a laser scanning microscope as shown in Fig. 1, in which 20 to 25 nuclei are visible from a cell culture. Low spatial resolution and the presence of breaks in tight junction structure of cells make the structural analysis of tight junction morphology a challenging biological problem. Therefore, we present a fully automated method for detecting nuclei, segmenting the tight junctions of each cell, and analyzing the cells with respect to the morphological structure of their tight junctions. We give the details of the technical approach in the next section. The data acquisition system and experimental results are presented in Section 3. Finally, we conclude in Section 4.

## II. Technical Approach

In our approach, we analyze the tight junction formation and integrity by following three main steps: (1) nucleus detection, (2) tight junction segmentation and skeletonization, and (3) feature extraction. We first localize each individual cell in the maximum intensity projection using thresholding, morphological operators and active contours. By using each nucleus position as a seed point, we automatically segment the tight junctions. Then, the skeletonization step generates the boundary of segmented

* Research sponsored by a seed grant from the Defense Threat Reduction Agency. This manuscript has been authored by employees of UT-Battelle, LLC, under contract DE-AC05-00OR22725 with the U.S. Department of Energy. Accordingly, the United States Government retains and the publisher, by accepting the article for publication, acknowledges that the United States Government retains a non-exclusive, paid-up, irrevocable, world-wide license to publish or reproduce the published form of this manuscript, or allow others to do so, for United States Government purposes.

Mahmut Karakaya, Ryan A. Kerekes, Jennifer L. Morrell-Falvey, Carmen Foster, and Scott T. Retterer are with Oak Ridge National Laboratory Oak Ridge, TN 37831 USA. E-mail: (karakayam@ornl.gov).

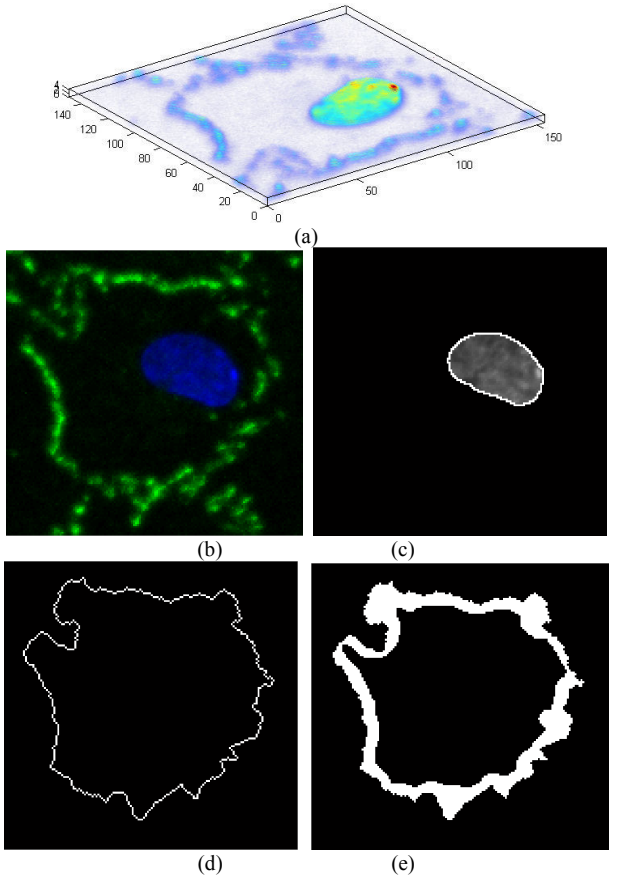


Figure 2. Representative figures of nucleus segmentation: (a) 3D image reconstruction of a nucleus and its tight junction cropped from a larger whole-field image shown in Fig. 1; (b) its maximum intensity projection of (a), where blue is nucleus and green is Z01; (c) nucleus segmentation result with highlighted boundary; (d) Final skeleton of tight junctions in (a); and (e) boundary regions.

tight junctions. Finally, features are extracted from each cell and its boundary to quantify the absence of tight junctions in the image. More details about these three steps are given in the following sections.

### *A. Nucleus detection*

Nucleus detection is essential to determine which tight junction segments belong to which cell. In our approach, we detect multiple nuclei in a low magnification maximum intensity projection using a combination of thresholding, grayscale morphology operators, and active contours.

The first step in nucleus detection is thresholding the maximum intensity projection of the nucleus channel of the image to separate the nucleus and background regions. Initially, the threshold value is determined by Otsu's histogram-based automatic thresholding method [3]. If this method does not produce a satisfactory result, the user can manually change the thresholding value to achieve a better thresholding result. After thresholding, connected component analysis labels all separate image regions as different nuclei using 8-connectivity, and the size of each nucleus is computed to eliminate the small, non-cellular particles.

Morphology operators shrink, enlarge and filter image regions based on a particular geometrical shape. Since the shape of a typical nucleus can be approximated as a disc, the image is first filtered by an erosion operator with a circular structuring element whose radius is equal to the size of the minimum volume enclosing the typical nucleus. By using each centroid as a seed point, an active contour algorithm automatically determines the boundary of each nucleus based on the Chan-Vese energy [4]. Fig. 2(a-b) shows a representative nucleus segmentation result of a cell cropped from the larger whole-field image shown in Fig. 1 and its maximum intensity projection, respectively. The resulting segmentation is used as the boundary of each nucleus as shown in Fig. 2c.

### *B. Tight Junction Segmentation and Skeletonization*

In order to segment the tight junction protein (ZO-1) from background, we need to make the following two assumptions. First, intensity values of tight junctions and nuclei are higher than intensity values of background and non-cellular materials. Second, each nucleus is surrounded by tight junctions. In an ideal segmentation case, an optimal threshold perfectly separates the cellular materials from the background and extracts the structure of the tight junctions for every cell. Since the distribution of the fluorescence material among different cellular regions is not uniform, the intensity values of tight junction segments are diverse in the optical sections. Moreover, the existence of background noise contributes to the difficult task to find the optimal threshold for tight junction segmentation. Therefore, we utilize a noise reduction algorithm and an active contour algorithm to segment the regions between the nucleus and tight junctions, which is called the cell body in the rest of the paper.

Since the distribution of background noise in the cell body can be approximated by Gaussian noise, the Wiener filter is a viable choice for noise reduction. Based on our second assumption, there is always a nucleus in the cell body. Therefore, each nucleus is used as a seed point for the active contour algorithm to automatically segment the cell body based on the Chan-Vese energy [4].

Tight junctions are formed across the paracellular space between adjacent cells as shown in Fig 2b. Skeletonization is a procedure that generates a unit-width line to represent tight junctions; thus, it is essential to simplify the analysis of morphological structure of the tight junctions. We utilize a modified version of the iterative 3-D skeletonization algorithm proposed in [5]. The original thinning algorithm iteratively peels the outermost layer of the binary image of the dendritic tree until only the central voxels of dendrites remain.

In this approach, the voxels which have the least number of neighbors are defined as the outermost layer and deleted first. Kerekes et al. [6] extended this approach by taking the intensity values of the corresponding voxels into account for the skeletonization of the grayscale segmentation image. Since the dimmest voxels in the outmost layer are deleted first, this approach keeps the brightest voxels of each tight junction in the initial skeleton. Fig. 2d shows the results of the skeletonization algorithm for tight junctions shown in Fig 2b.

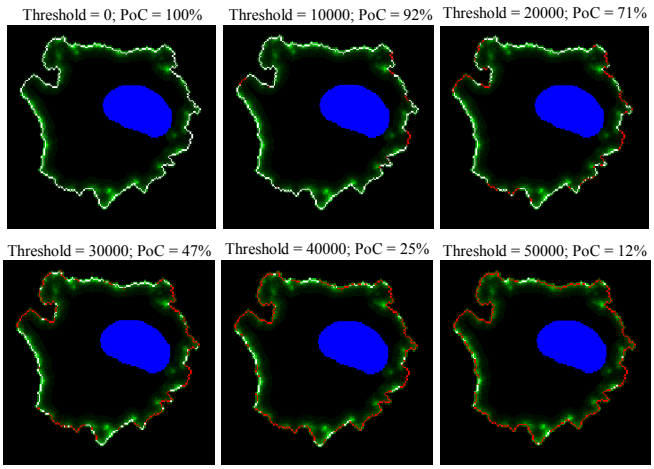


Figure 3. Illustration of feature extraction for percentage of continuity (PoC) of tight junctions in boundary region (shown in Fig. 2e). Breaks are labeled as red and continuous boundary is labeled as white.

In order to extract features from cells, we first need to define the boundary region for each cell. We define each segmented cell body as the inner boundary of its boundary region and each cell periphery as the outer boundary for the cell. Therefore, the boundary region for each cell is defined as the area between inner and outer boundary as shown in Fig. 2e.

### C. *Feature Extraction*

In order to analyze the tight junctions, we extracted the following features from each cell: (1) number of nuclei, (2) area of each nucleus, (3) peripheral length of tight junctions, (4) ZO-1 intensity at the tight junctions, (5) percentage continuity of tight junctions, (6) number of breaks in tight junctions, and (7) average length of breaks in tight junctions.

Continuity of tight junctions around the periphery is essential in assessing the extent of tight junction formation and integrity which is indicated by ZO-1 intensity at the boundary region being higher than the defined threshold. If the ZO-1 intensity at any part of the boundary region drops below the defined threshold, it is defined as a break along the cell periphery. Fig. 3 illustrates the feature extraction for percentage continuity of tight junctions in boundary region at various ZO-1 threshold values.

## III. Data and Experimental Results

### A. *Data acquisition*

Human umbilical vein epithelial cells (HUVEC) were grown to confluence on fibronectin coated coverslips and prepared for microscopy using DAPI to detect nuclei and anti-Z0-1 antibodies (Invitrogen) to detect tight junctions. Images were collected using a Zeiss LSM710 confocal laser scanning microscope. Optical sections were collected at 0.5 µm step-size increments and processed as a maximum intensity projection using Zeiss Zen 2009 software. Images were collected using either a 20x or 40x objective, with approximately 20-200 cells in each field. Each volume is approximately 512x512x5 voxels in size.

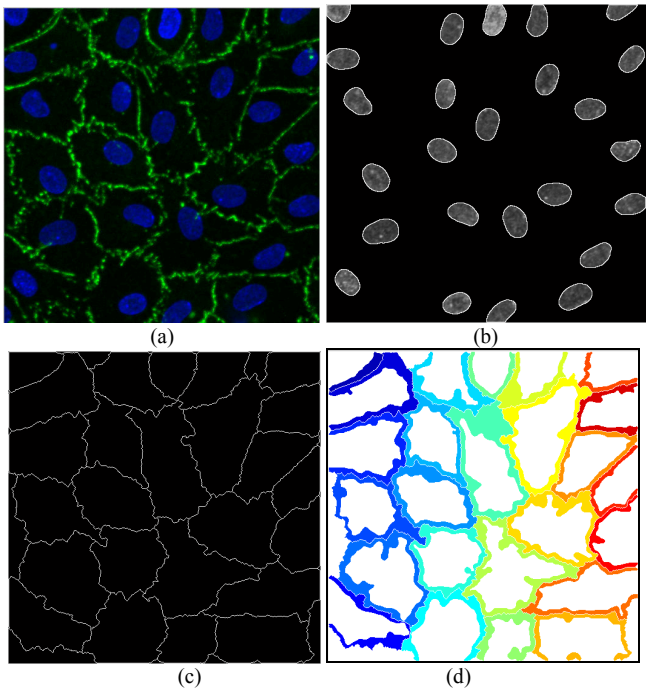


Figure 4. (a) Maximum intensity projection of the whole-field image shown in Fig.1, (b) Each segmented nucleus, (c) Final skeleton of tight junctions in (a) and (d) Boundary regions of each cell.

### B. *Experimental Results*

In this section, we show test results from applying our proposed algorithm to multiple cells in large-scale 3D image stacks. In two experiments, we tested our automatic nucleus detection and tight junction segmentation algorithms. The first dataset (HUVEC_anti-ZO-1_DAPI-2) contains 3D image stacks collected as described in the data acquisition section above with the higher zoom factor. There was no available ground truth for these datasets.

The maximum intensity projection of the whole-field images, nucleus detection results, tight junction segmentation and skeletonization results of the first image volume are shown in Fig. 4 (a-d), respectively. We observe that each nucleus is detected and segmented precisely; thus the skeletonization and boundary region segmentation appears to be accurate.

After determining the final boundary regions, we extract the features from the first data set shown in Fig. 4a. Fig. 6a shows the average percentage continuity of tight junctions. We observe as expected that the average percentage of peripheral continuity decreases as the ZO-1 threshold value increases. The total number of breaks in tight junctions is shown in Fig. 6c, and we observe that the total number of breaks in tight junctions first increases and then decreases as the ZO-1 threshold value increases. This happens because as the length of each break increases, sometimes multiple small breaks merge and become a long break. In Fig. 6e, we observe that the average length of breaks in tight junctions increases as ZO-1 threshold value increases.

In the second experiment, we test our proposed algorithm with the larger whole-field image stacks (HUVEC_anti-ZO-1_DAPI-1). The maximum intensity projection of the

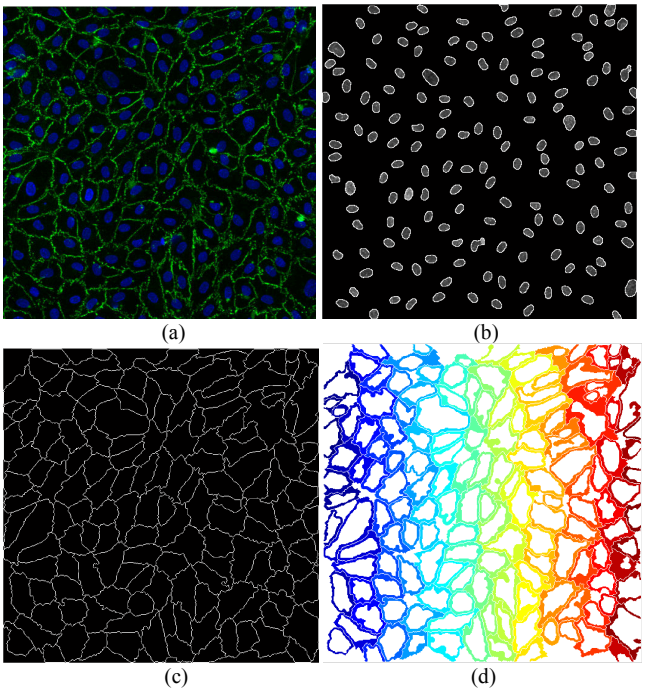


Figure 5. (a) Maximum intensity projection of the whole-field image, (b) Each segmented nucleus, (c) Final skeleton of tight junctions in (a) and (d) Final boundary regions of each cell with different colors.

whole-field images, nucleus detection results, tight junction segmentation and skeletonization results are shown in Fig. 5 (a-d), respectively. By close manual inspection, we observe that each nucleus is detected and segmented with high precision; thus, the skeletonization and boundary region segmentation exhibits high accuracy.

After determining the final boundary regions, we extract the features from the data set. Fig. 6b shows the average percentage continuity of tight junctions. We observe similar trends to those in the first experiment, specifically that the average percentage of peripheral continuity decreases as ZO-1 threshold value increases, the total number of breaks in tight junctions increases and then decreases, and the average length of breaks in tight junctions increases as ZO-1 threshold value increases. These results for the second experiment are depicted in Figs. 6b, 6d, and 6f.

## IV. Conclusion

In this project, we studied segmentation of tight junctions and analyzed tight junction formation and integrity in 3D confocal images. Here we presented a three-step processing algorithm to analyze tight junctions. In our approach, we first localize each individual nucleus in the image by using morphological filters and active contour. By using each nucleus position as a seed point, we automatically segment the cell body based on the active contour. We then use intensity-based skeletonization algorithm to generate the boundary regions for each cell, and features are extracted from tight junctions of each cell for disruption analysis in tight junctions. Based on qualitative results and quantitative

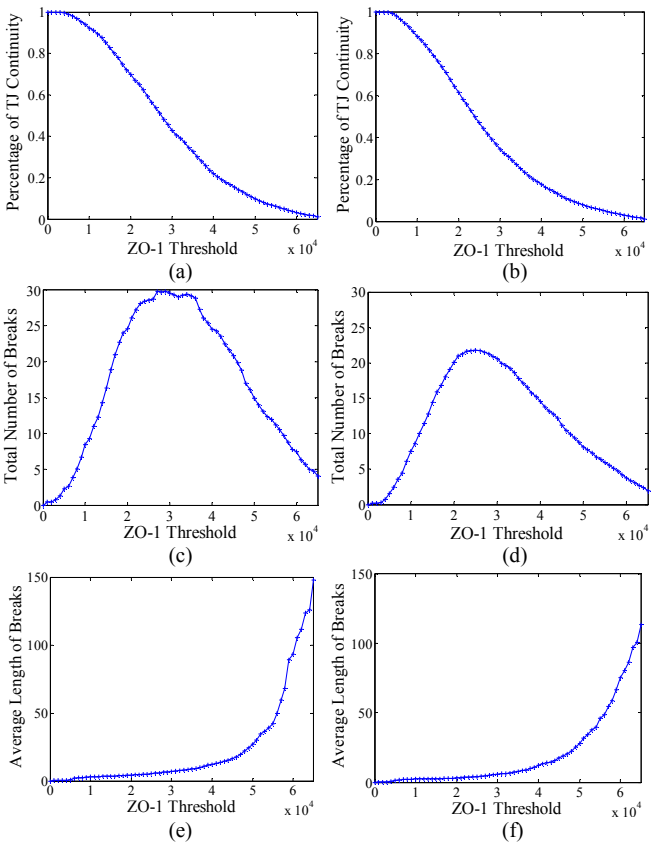


Figure 6. Results for the first and second experiments, respectively. (a-b) Average percentage continuity of tight junctions, (c-d) average number of breaks in tight junctions, and (e-f) average length of breaks in tight junctions.

comparisons, we show that we are able to automatically segment tight junctions and compute relevant features that quantitatively measure the Z01 concentration and continuity between cells. Ground truth was not available to properly validate our algorithm; however, larger-scale validation using electrical conductivity measurements across the cells represents a possible direction for future work. Nonetheless, we believe that our proposed approach represents a useful tool for future statistical analysis of tight junction formation and integrity.

## References

[1] K. Matter, and M. S. Balda, "Functional analysis of tight junctions", Methods, vol. 30(3) pp. 228-234, 2003.

[2] H. Wan and et al., "Der p 1 facilitates transepithelial allergen delivery by disruption of tight junctions". Journal of Clinical Investigation vol. 104 pp. 123–133, 1999.

[3] N. Otsu, "A threshold selection method from gray-level histograms". IEEE Trans. Sys., Man., Cyber. vol. 9 (1): pp. 62–66, 1979.

[4] T. F. Chan, and L. A. Vese, "Active contours without edges," IEEE Transaction of Image Processing, vol. 10(2), pp. 266-277, 2001.

[5] X. He, E. Kischell, M. Rioult, and T. J. Holmes, "Three-dimensional thinning algorithm that peels the outmost layer with application to neuron tracing," Journal of Computer-Assisted Microscopy, vol. 10(3), pp. 123-135, 1998.

[6] R. A. Kerekes, S. S. Gleason, R. A. P. Martins, and M. Dyer, "Fully automated segmentation and characterization of the dendritic trees of retinal horizontal neurons," BSEC 2010: Annual ORNL Biomedical Science and Engineering Conference, May 2010.